

Ultrasound phase-contrast transmission imaging of localized thermal variation and the identification of fat/tissue boundaries

G T Clement and K Hynynen

Department of Radiology, Harvard Medical School, Brigham and Women's Hospital,
75 Francis St. Boston, MA 02115, USA

E-mail: gclement@hms.harvard.edu

Received 11 November 2004, in final form 20 January 2005

Published 22 March 2005

Online at stacks.iop.org/PMB/50/1585

Abstract

We present a new ultrasound technique for registering localized temperature changes in soft tissues. Conversely, small temperature changes may be induced in order to image tissue layers. The concept is motivated by the search for a compact, low cost method for guiding noninvasive thermal therapies; however its utility may extend to a wide range of imaging problems such as tumour imaging in the breast. This method combines ultrasound transmission imaging, planar projection techniques and phase-contrast theory. After outlining the theoretical foundation of the technique, its feasibility is tested by simulating localized heating within homogeneous tissue layers. Success of this imaging method is evaluated as a function of the ultrasound-imaging wavelength for a Gaussian-shaped heated region over the frequency range from 0.1 to 2 MHz. Furthermore we simulate two-dimensional image reconstruction from a receiving array. We conclude that thermal phase-contrast imaging in tissues is plausible for detecting the treatment spot in thermal therapies while operating at frequencies below 1 MHz. Additionally, it may also be possible to use the method for noninvasive thermometry. However, thermometry would require operation at higher frequencies at the tradeoff of increased attenuation and higher sensitivity to scattering, which needs to be further explored.

(Some figures in this article are in colour only in the electronic version)

1. Introduction

A number of minimally invasive thermal therapies are being studied as an alternative to radical surgery and radiation therapy in treating cancer. These methods include focused ultrasound surgery, RF-ablation and laser surgery. Benefits of these procedures include reduced recovery time, a smaller risk of complications, lower rates of infection and reduced need for general

anaesthesia. Both laboratory and clinical experience (Stepanow *et al* 1995, Pomeroy *et al* 1995) have shown that the energy delivery during thermal procedures must be monitored during these treatments in order to assure accurate energy delivery. Ultrasound (Fry *et al* 1968, Sanghvi *et al* 1999, Sheljaskov *et al* 1997, Chapelon *et al* 1999) CT (Fallone *et al* 1982, Jenne *et al* 1997), and magnetic resonance imaging (MRI) (Cline *et al* 1995, Quesson *et al* 2000, McDannold and Jolesz 2000) have all been used for this feedback. All these methods may also offer the ability to detect the induced temperature elevation (McGough *et al* 1994, Maas-Moreno and Damianou 1996, Maas-Moreno *et al* 1996, Dewey 1994), but only MRI has been shown to work accurately *in vivo*.

We examine here the plausibility of an ultrasound phase-contrast method for imaging localized temperature rises, such as those experienced in thermal-ablative treatments. This numeric study is motivated by images that we previously obtained using an acoustic camera imaging system (King *et al* 2003). In this past study we observed a reversible, time-dependent variation in image intensity in the region of the therapeutic sonications in bovine fat and porcine and rabbit livers. Our present hypothesis is that this image variation was due to a phase variation in the imaging field, which is exploited in the phase-contrast imaging approach. The ability to use an ultrasound for thermal monitoring could potentially provide a very low cost, compact and sensitive monitoring method.

On the basis of the results of our present study, we additionally indicate that the method may have utility in tissue identification. That is, the differences in temperature dependence on the speed of sound (and inversely ultrasound phase) could be exploited to identify tissue type in a region that is globally heated by several degrees. The difference between tissue sound speeds is particularly strong in the case of muscle and fat layers, such as those present in human female breast tissue. Further, we note that the method could also be used to identify heat capacity and perfusion, by measuring cooling as a function of time after uniform heating of a given region.

A temperature rise of just 1 °C in tissue can typically alter its sound speed by about 5 m s⁻¹. This can potentially cause significant phase distortion in any probing ultrasound beam, with a dependence on the size of the heated area and the frequency of the ultrasound. To interpret this distortion, we consider phase-contrast imaging (Hecht 1987), which has been used extensively in optical applications to detect objects or disturbances that have transmission characteristics similar to their surrounding medium but slightly different wave speeds. The approach relies on complete transmission through the tissue, so its applicability is limited to targets such as the breast where ultrasound can be produced and detected by different transducers. Although intensity-based transmission images are well documented, the method's potential for imaging small localized phase shifts, such as those used in acoustic thermometry (Wadley *et al* 1986, Seip and Ebbini 1995), has not been exploited.

Previous application of transmission ultrasound has been suggested for developing orthographic ultrasound images (Green *et al* 1973, Fry and Jethwa 1974, Hentz *et al* 1987, Lehman *et al* 2000) in ultrasound transmission tomography (Carson *et al* 1977, Dines *et al* 1981, Opielinski and Gudra 2000) and in reflex transmission imaging (Green and Arditì 1985, Green *et al* 1991). Transmission acoustic camera systems have demonstrated this imaging in real-time or near-real-time (Green *et al* 1973, Metherell *et al* 1970, Whitman *et al* 1972, Lasser *et al* 1996, Ermert *et al* 2000, Lasser 1997). Specific examples of transmission imaging in tissue include measurement of the attenuation properties of tissues (Marich *et al* 1975a, 1975b, Zatz 1975, Weigel and Cartee 1983, Hentz *et al* 1987, Wells 2000), as well as demonstration of the ability to image lesions in the breast (Lehman *et al* 2000). The primary requirement for tissue imaging is a window where ultrasound may pass through the object to be imaged.

We expect that imaging thermal variation with phase-contrast transmission ultrasound can achieve a more intense signal-to-noise ratio (SNR) than backscattered ultrasound due to the phase-contrast method's strong phase sensitivity versus the low reflection coefficient caused by temperature changes. Here we test the method's ability to produce thermal images by simulating the signal from a planar transmission source and a 1-D receiving array. We also indicate its ability to identify fat and muscle layers. With real-time acquisition, it is conceivable that localized or time-dependent phase shifts, including those that occur in tissue during thermal therapies, could be imaged and quantified. Such distortions have been studied and quantified (O'Donnell and Flax 1988, Nock *et al* 1989, Liu and Waag 1994, Hinkelman *et al* 1995, Zhu and Steinberg 1997), but have been generally viewed as a source of beam aberration.

2. Theory

2.1. Forward propagation

Transmission signals are sensitive to changes in both sound speed and attenuation. Both of these properties can be exploited for imaging. The former property is considered in the present study to image thermally induced sound speed changes, while the latter has been previously examined as a method for detecting and measuring thermally coagulated tissues (Clement *et al* 2001). In general, variation in absorption and sound speed can occur simultaneously, but phase (sound speed) imaging is discussed separately here to illustrate its possible utility in thermal monitoring. The theory outlined below assumes the heating effects are too small to produce a permanent change in tissue, representing heating by small 'test' amounts, which would be performed to locate or verify a focal location.

The theory first considers a pressure field $p(x, y, z, t)$, given in standard Cartesian coordinates, which encounters a localized temperature variation contained within a volume of radius R . The sound speed in this volume will change as a function of temperature $c(T(x, y, z))$ that will be dependent on the tissue type. In the present case, it is assumed that the tissue within the heated volume is homogeneous. Immediately after the propagating through the region, the field over the plane at z_0 will be shifted in phase by the amount

$$\Delta\Phi(x, y, z_0) = k_0 \int_{-R}^R [\alpha(x, y, z) - 1] dz \quad (1)$$

relative to an unperturbed field within the region for a given wavenumber $k_0 = \omega/c_0$, baseline sound speed c_0 (presently assumed to be homogeneous) and a phase distortion $\alpha = c_0/c(x, y, z)$. If the region experiences only a change in sound speed (neglecting absorption changes), $\Delta\Phi(x, y; z_0)|_{x, y < R}$ will be purely real. Temperature rises at the focus of a therapeutic transducer, illustrated in figure 1, are modelled with this approach.

2.2. Image reconstruction

Assuming a phase shift given by equation (1), image reconstruction requires two steps. The signal must be propagated backwards from the source to the plane at z_0 in order to reconstruct $\Delta\Phi$ as closely as possible, given limitations imposed by noise and the spatial bandwidth of the signal. Second, equation (1) must be inverted to solve for α as a function of position. Two separate methods are proposed for reconstructing $\Delta\Phi$: the first approach (analysis method) back-propagates the signal to planes close to the temperature distribution and tomographically reconstructs the temperature profile, using the propagated planes as

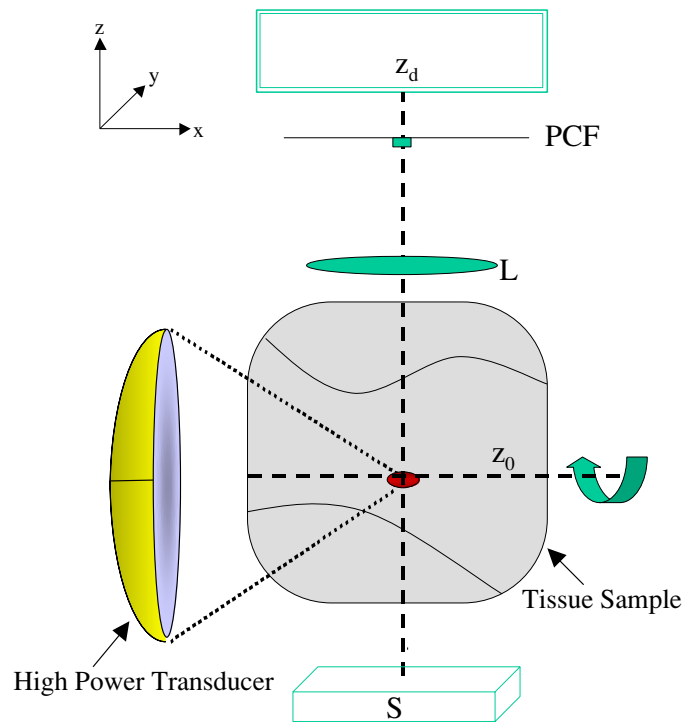


Figure 1. Experimental setup.

integral projections. The second method (hardware approach) uses a phase-contrast filter, which would be used in conjunction with an acoustic lens. Since the filtering method requires a lens it would be more susceptible to attenuation at higher frequencies and would be limited to temperatures inducing small phase shifts, as addressed below. However it could be easily added to existing transmission imaging devices, providing real time images, without additional signal processing.

2.3. Backward projection technique

The backward projection method (Stepanishen and Benjamin 1982) is an angular spectrum approach that uses a transfer function in wavevector-frequency space to numerically propagate the signal at the receiver backward to a plane directly beyond the heated region. This signal is compared to a reference signal acquired before heating. The field over the plane z_0 is related to the field at any other plane z by a wavevector-space (k -space) transfer function that, in a linear homogeneous medium, only changes the signal phase. When strong attenuation or tissue layers with strong impedance mismatches are considered in the media, the transfer function must be modified (Schafer *et al* 1987, Schafer 1988). These corrections are neglected in the present discussion. Their omission is considered reasonable based on a previous experimental study with an acoustic camera [20], which demonstrated the ability to transmit ultrasound to image in tissue at frequencies above 7 MHz without severe distortion. It is expected that the lower frequencies used here (below 2 MHz) will accordingly be less susceptible to distortions.

2.4. Phase-contrast filter

The acoustic filter described here would allow images to be acquired without the use of the numerical back-projection. This lensing technique could make real-time imaging possible with receiving arrays that are only sensitive to time-averaged field intensity. However, this technique would have a decided drawback at high frequencies due to signal attenuation in the lenses. The system described below is a direct analogue to phase-contrast optical filtering systems designed for acousto-optic measurements. Such methods were used by Clement (Clement and Letcher 1999, Clement 1999) to image highly localized and diffraction-limited acoustic fields and more recently by Pitts *et al* (Pitts *et al* 2001) for reconstructing wideband fields over a large field of view. It is not necessary to measure the full acoustic pressure if an acoustic lensing and filtering system is introduced, but rather it is sufficient to measure the time-averaged acoustic intensity at the detector (Lasser 1997).

Similar to the backward projection technique, the model considers a planar source placed parallel to a receiving array as depicted in figure 1, but additionally requires an acoustic lens (L) be placed along the acoustic axis, which focuses the beam such that a localized inhomogeneity at the imaging plane (O) will be projected onto the receiving plane (I). The acoustic lens is assumed to be a simple bi-convex system and is modelled using the Eikonal equations. Banerjee and Poon (Banerjee and Poon 1991) outline a detailed account of the focusing properties of these lenses. By the principles of Fourier optics for a biconvex lens (Goodman 1968), it can be shown that the field in the focal plane (F) will be proportional to the *spatial* Fourier transform of equation (1), but with a phase curvature introduced by the lenses

$$\begin{aligned} \tilde{P}(x, y, z_f; \omega) &= \frac{i\omega}{2\pi c_0} \exp\left(-i\frac{\omega}{c_0}(z_0 - z_f)\right) \exp\left(-i\frac{\omega}{2c_0 z_f} \left(1 - \frac{z_0}{z_f}\right) (x^2 + y^2)\right) \\ &\times \int P(x', y', z_0; \omega) \exp\left(-i\frac{\omega}{c_0} \left(\frac{x}{z_f} x' + \frac{y}{z_f} y'\right)\right) dx' dy'. \end{aligned} \quad (2)$$

Here P is the field after being phase shifted as specified by equation (1) and z_f is the axial location of the focal plane. This field may be spatially Fourier transformed and propagated to the image plane (Forbes *et al* 1991) so that

$$\begin{aligned} p(x, y, z_R, \omega) &= \frac{1}{2\pi} \iint \tilde{P}(k_x, k_y, z_0, \omega) \\ &\times \exp\left(i(z - z_0) \sqrt{\frac{\omega^2}{c^2} - k_x^2 - k_y^2}\right) e^{i\omega t} e^{ik_x x} e^{ik_y y} dk_x dk_y. \end{aligned} \quad (3)$$

The temporal inverse transform of equation (3) then gives the time-dependent field $p(x, y, z_R, t)$, where the transient average intensity recorded by the receiver is

$$I(x, y) = \frac{1}{\rho c_0 T} \int_0^T p(x, y, z_R, t)^2 dt, \quad (4)$$

where T is the persistence time of the receiver.

The study considered a 20 mm diameter circular planar source transducer operated in a continuous-wave mode. Frequencies between 0.1 MHz and 2 MHz were separately modelled. A modified impulse response approach (Stepanishen 1971) was used to generate the field. Simulated fields were propagated over the 10.0 cm region between the object and the transducer face. A localized Gaussian-shaped heated region was then created, causing a transformation of the field as expressed by equation (1).

The initial simulations reconstructed heating within a completely homogeneous tissue for the purpose of determining the method's spatial and thermal resolution. A Gaussian

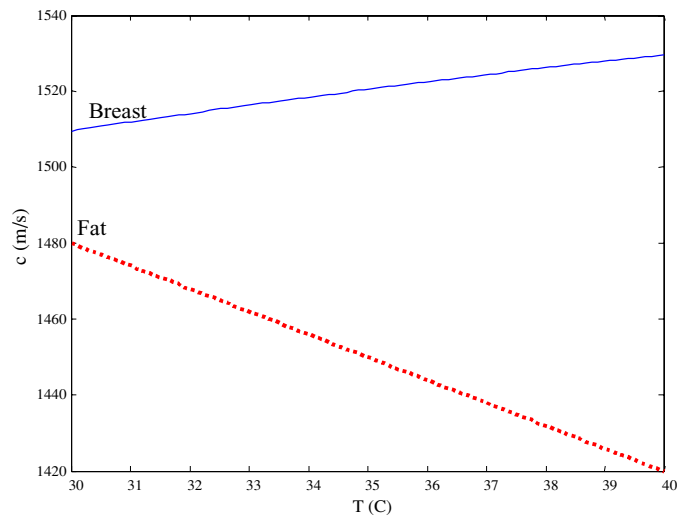


Figure 2. Temperature dependence of fat and breast tissue sound speeds, showing an increase in sound speed in tissue, and a decrease in fat.

heating profile and a circular heating pattern, mimicking that of a focused ‘vortex’ radiator (Umemura and Cain 1989) were simulated. These heating patterns are representative of those that could be used in thermal therapies in the breast. The FWHM of the Gaussian and the equivalent width of the vortex heating pattern was held constant and the imaging frequency varied in order to obtain the accuracy of the reconstruction relative to the ultrasound wavelength. Both heating profiles were reconstructed with the FWHM of the temperature distribution equal to $\lambda/16$, $\lambda/8$, $\lambda/4$, $\lambda/2$, λ and 2λ after the tissue was heated by a peak magnitude of 5°C . Breast tissue sound speed as a function of temperature, shown as the solid line in figure 2, was determined from data compiled by Duck (Duck 1990), while the skin sound speed was assumed to be a constant value of 1400 m s^{-1} .

To examine the effects of noise and inhomogeneity on the reconstruction, a series of simulations were performed where pseudo-random noise was added to the signal before projection. In these simulations, the 5°C heating was simulated as described above in a region containing an interface between breast and fat tissue. In one set of reconstructions a uniformly distributed pseudo-random data set was generated for each projection angle, in order to represent random ‘white’ noise in the signal. In a second set of reconstructions a single, normally distributed pseudo-random data set was generated and added to the sound speed to simulate small variation across the tissue. In all cases, the signal-to-noise ratio of the reconstructed speed-of-sound image was determined in both the breast and fat tissue and the ability to perform the reconstruction assessed.

For each simulation, the field was sectioned into a 450×450 speed-of-sound matrix through which the pressure field was propagated. A line along each image plane then represents a linear array consisting of 450 elements over a linear distance of 100 mm. To reconstruct two-dimensional slices of the temperature field, k -space reconstruction is performed using images acquired at regular intervals 180° around the sample. Eighteen images are acquired for reconstructions in homogeneous tissues and 45 for images in the simulated breast tissues described below. The reconstruction presently applied is performed with a lowpass spatial frequency filter with a cutoff frequency where $k \leq \omega/c$. The method is the same regardless of whether the data were obtained from the back-projection method or with the phase-contrast

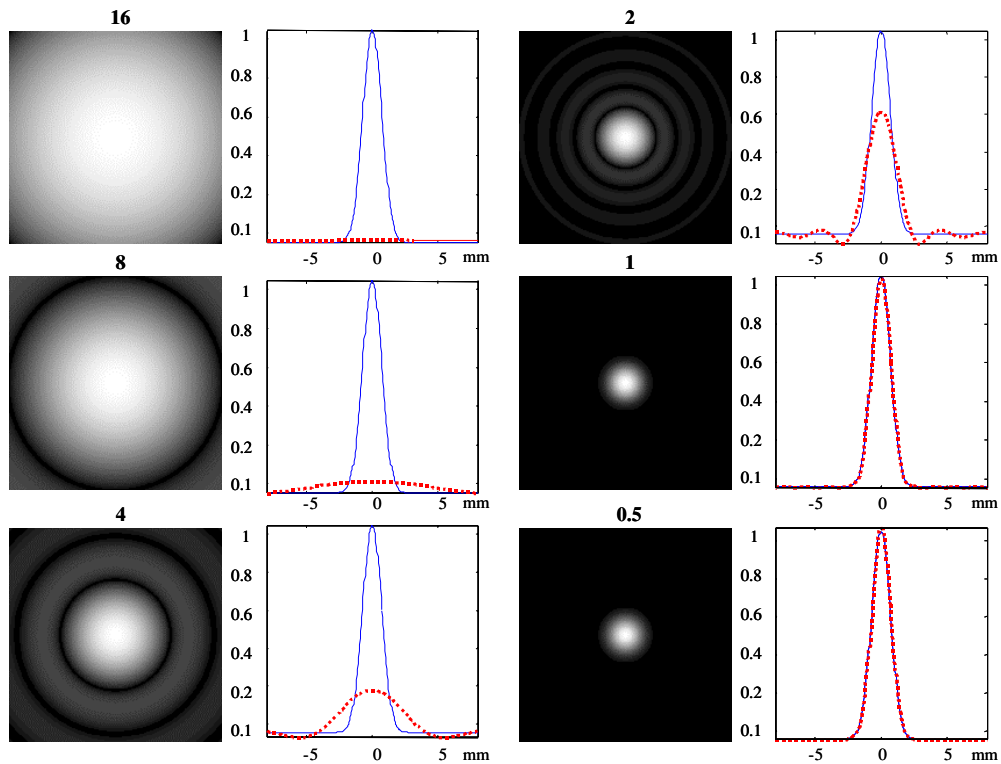


Figure 3. Imaging of a Gaussian-shaped temperature rise in tissue. Images (right) and their normalized cross-sections (left) for a series of wavelengths from $16\times$ to $0.5\times$ the FWHM of the heating profile. In the cross-sections the apparent heating (dotted) is compared with the actual heating profile (solid).

filter, and is similar to methods used for diffraction reconstructions (Kaveh *et al* 1984). Due to the large angle of rotation required, this reconstruction tomography would only be applicable for the breast, the testicles or other areas such as the brain that could be accessed over a reasonably wide range of angles.

3. Results

3.1. Heating in homogeneous tissue

Results of the Gaussian heating inside homogeneous tissue are presented in figure 3. The figure shows intensity plots of the reconstructed thermal images (R) as well as radial cross-sections of the actual temperature profile and the reconstruction (L). The reconstruction algorithm was able to identify the heating profile when ultrasound wavelength was smaller than or equal to the FWHM of the temperature profile. When the wavelength was twice the object's FWHM, heating was still detected, but the perceived temperature was $2.0\text{ }^{\circ}\text{C}$ less than the actual peak temperature and the image was distorted, giving an apparent FWHM $1.6\times$ the size of the actual. At $1/4$ wavelength, the reconstructed profile's apparent FWHM increased to $3.1\times$ the actual profile's width and the apparent temperature peak was only $0.70\text{ }^{\circ}\text{C}$. By $1/8$ the wavelength, the detected temperature rise is less than 10% of the actual value and the heating profile bears

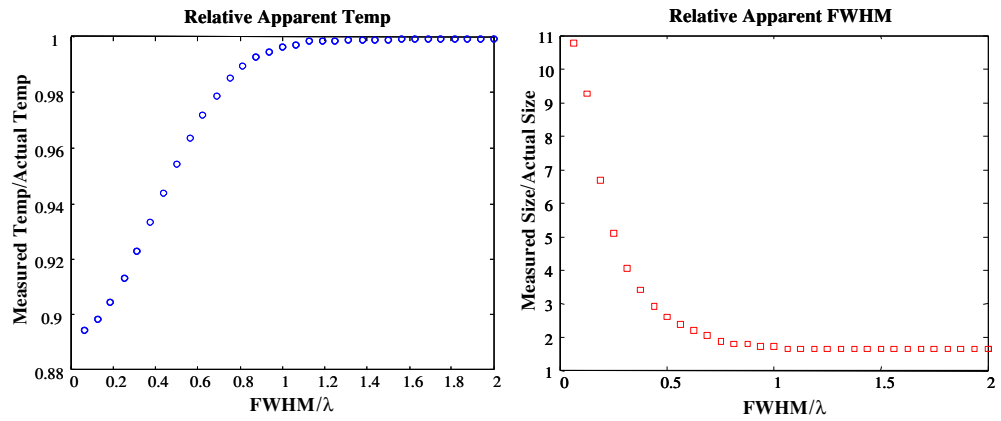


Figure 4. Apparent temperatures (right) and FWHM of heated area (left) with increasing FWHM relative to imaging wavelength.

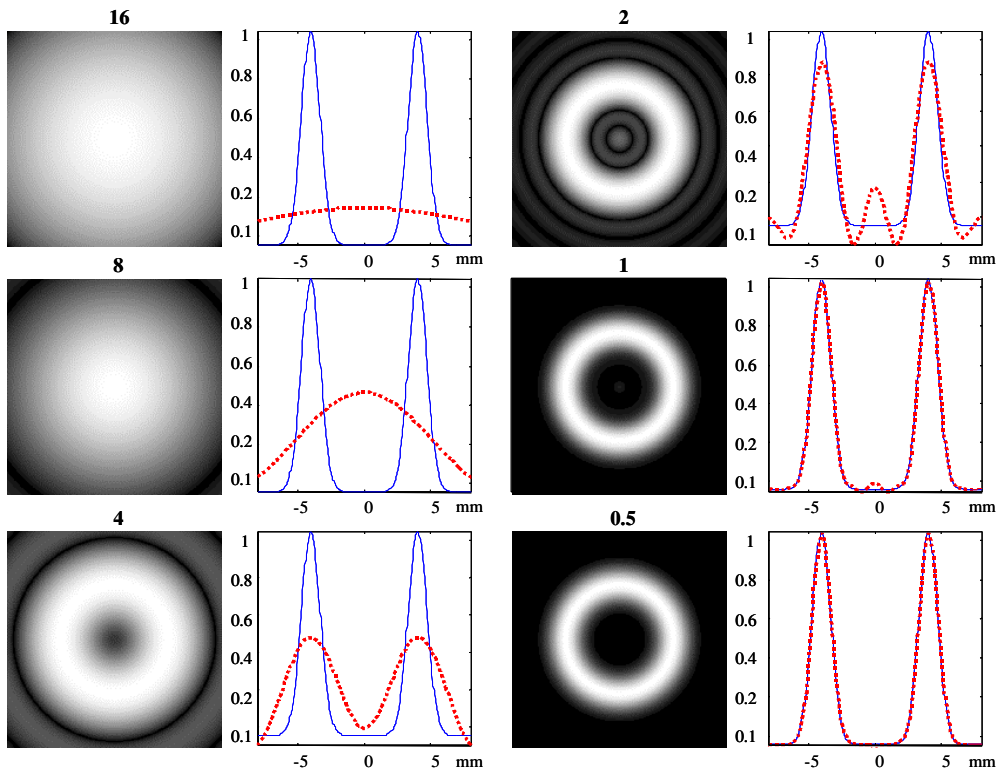


Figure 5. Imaging of a ring-shaped temperature rise in tissue. Images (right) and their normalized cross-sections (left) for a series of wavelengths from $16\times$ to $0.5\times$ the FWHM of the ring thickness. In the cross-sections the apparent heating (dotted) is compared with the actual heating profile (solid).

no resemblance to the actual case. This trend towards underestimating the temperature rise and overestimating the FWHM values is illustrated in figure 4. Figure 4(a) shows a plot of

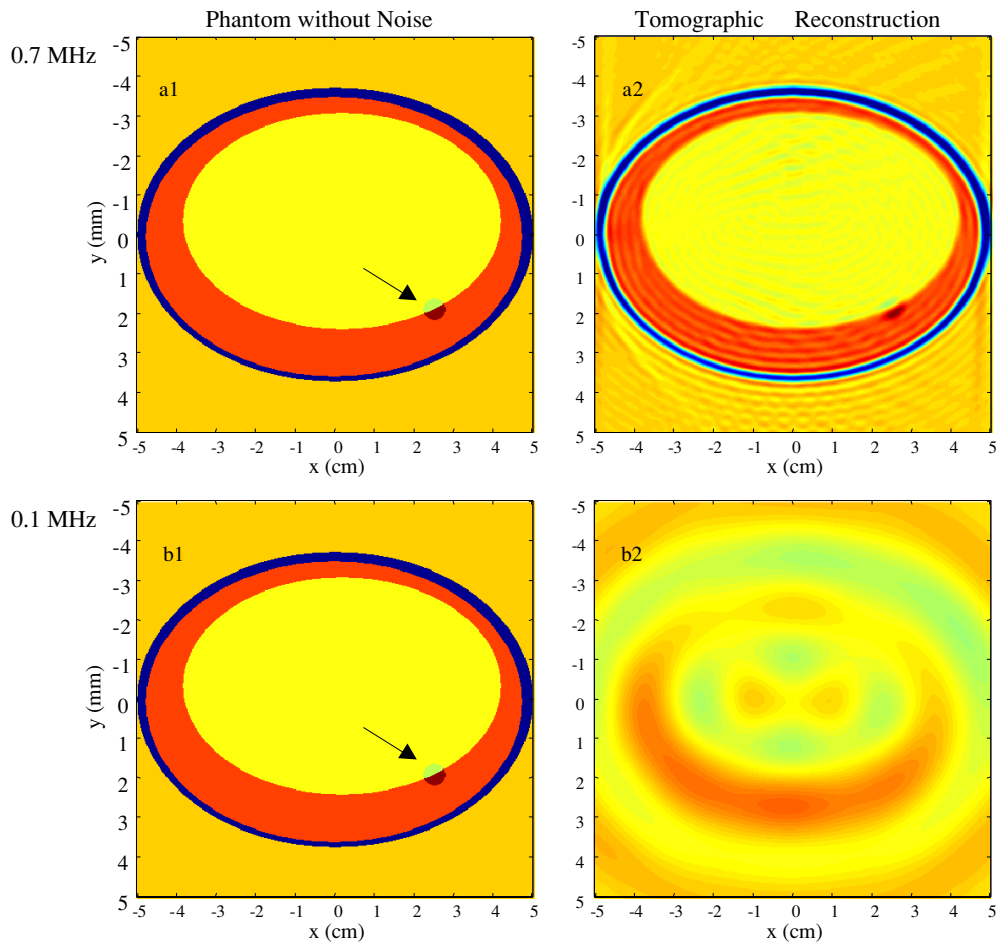


Figure 6. (a1), (b1) A tissue phantom consisting of outer skin, fat, and a central tissue layer is heated 5 C at the fat-tissue interface and reconstructed at 0.7 MHz (a2) and 0.1 MHz (b2).

the apparent temperature rise normalized to the actual temperature rise as a function of the FWHM normalized to the actual. Similarly, Figure 4(b) shows the normalized apparent size of the heated region.

Similar simulations were performed for the ring-shaped vortex heating pattern, resulting in the reconstruction shown in figure 5. When the ultrasound wavelength was smaller than the diameter of the ring ($5 \times$ the heating half-maximum width), the reconstruction was able to reproduce a ring-shaped, albeit distorted, pattern. However when the wavelength was larger than the full diameter of the ring, the heated region incorrectly appeared to have its highest temperature at the centre of the region. Similar to the Gaussian heating pattern, the image was fully reconstructed using a wavelength equal to, or smaller than the ring's half-maximum width.

3.2. Inhomogeneous tissue

The second simulation attempted to identify a heated region within a modelled tissue phantom consisting of skin, muscle and fat layers. The first goal of the reconstruction was to

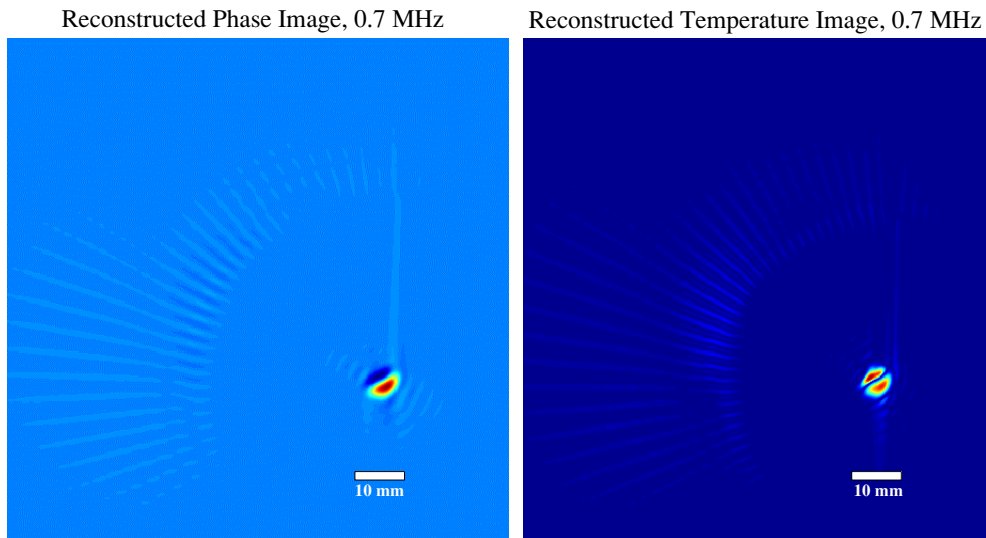


Figure 7. Phase (left) and temperature (right) images of a 5 °C heated region at a fat-tissue interface.

differentiate between layers of water, fat and tissue within the breast and then to use the data for reconstructing the image. In a highly inhomogeneous tissue such as the breast, the phase distortion caused by heating cannot necessarily reconstruct the heated region unless the composition of the tissue is known *a priori*. To minimize refraction while providing a reasonable spatial resolution, a low operating frequency of 0.4 MHz was chosen. A 5 °C temperature rise was induced uniformly throughout a 5 mm-diameter cylindrical volume, and the sound speed was adjusted according to the tissue type at a specific point in the volume with a resolution of 0.2 mm³. The tissue and fat sound speeds as a function of temperature are presented in figure 2.

Using the observations of the reconstructed sound speed variation in homogeneous tissues from heating, it was believed that full temperature reconstruction would be possible if the imaging wavelength is equal to, or smaller than the FWHM of the heating profile. Based on this observation, imaging within tissue layers was simulated at 0.1 MHz, 0.4 MHz and 0.7 MHz, representing images below, at and above the frequencies necessary for the application of the proposed reconstruction. Figure 6(a1) shows skin (outer), fat (middle) and tissue (centre) layers with a 5 mm-diameter heated region in the interface between the fat and tissue later. The result of reconstruction of the 0.7 MHz signal is presented in figure 6(a2). The same model (figure 6(b1)) was used as the starting point to simulate the 0.1 MHz propagation and reconstruction shown in figure 6(b2), which fails to locate both the tissue interfaces and the heating. Direct image subtraction from an image of the unheated tissue results in the images presented in figure 7, showing the phase-contrast reconstruction (left) and the associated thermal image (right) based on identification of the tissue as fat or tissue. A comparison of the reconstruction profiles across the centre of the heated region is given for 0.1 MHz, 0.4 MHz and the 0.7 MHz reconstructions in figure 8. In all cases, including heating in tissue, fat and both simultaneously, the approximate size of the heated region was correctly identified by the 0.4 MHz, and 0.7 MHz signals. However, all cases registered some error in identifying the temperature change of the heated region, with the most accurate profile and values occurring at 0.7 MHz.

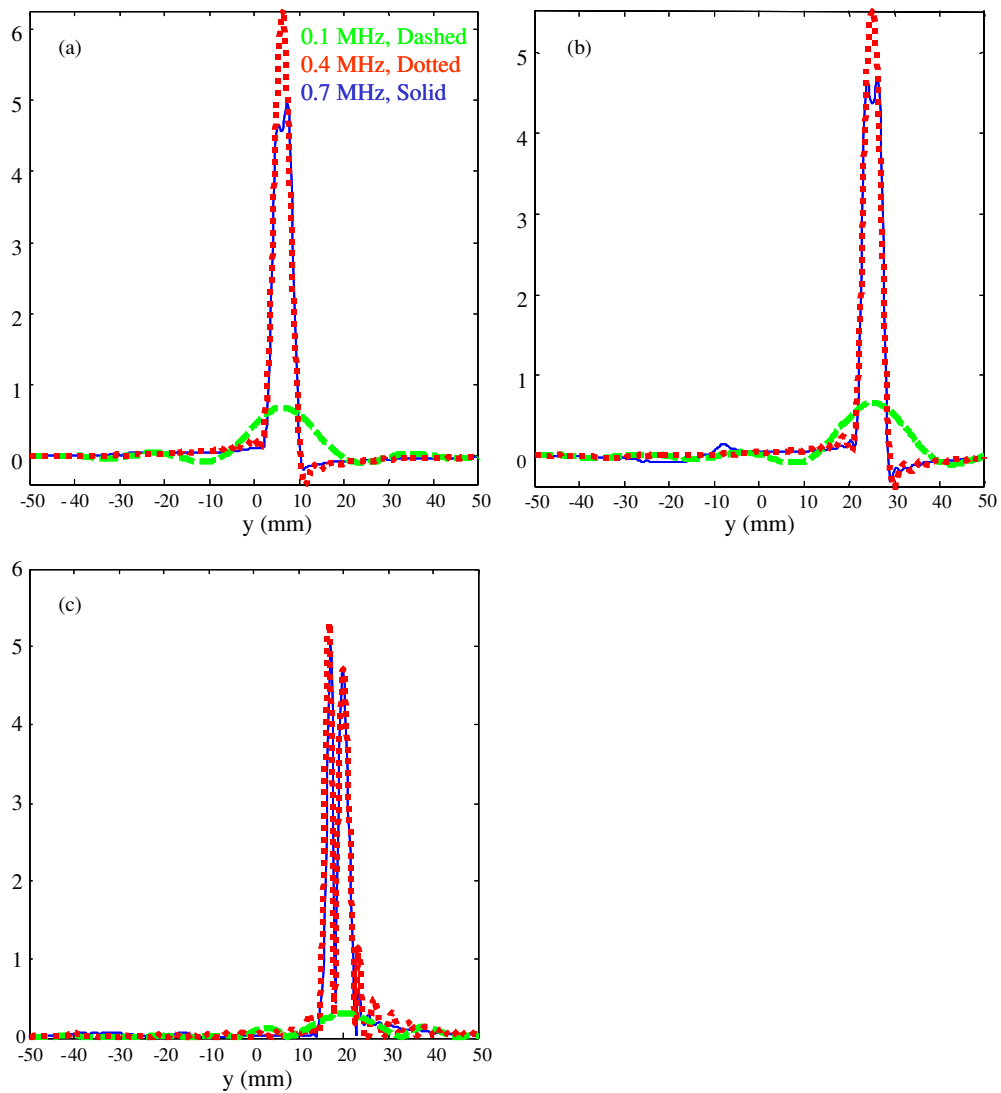


Figure 8. Cross-section of apparent temperature in tissue layer (a), fat layer (b) and interface (c) of a tissue phantom at 0.1 MHz, 0.4 MHz and 0.7 MHz.

Simulation of the heating at the tissue interfaces was next repeated at 0.7 MHz, but with noise added to the signal. Varying levels of uniformly disturbed white noise and Gaussian noise were used to determine the stability and limits of the method in a noisy environment. Figure 9(a1) shows layers with a 5 mm-diameter heated region in the interface between the fat and tissue later in the presence of time-varying white noise and figure 9(a2) shows its tomographic reconstruction. Reconstruction of the same signal, but with a constant level of Gaussian noise (figure 9(b1)) is presented in figure 9(b2). A series of reconstruction profiles across the centre of the heated region is given for both noise types with decreasing SNR in figure 10, demonstrating stability under a modest noise level.

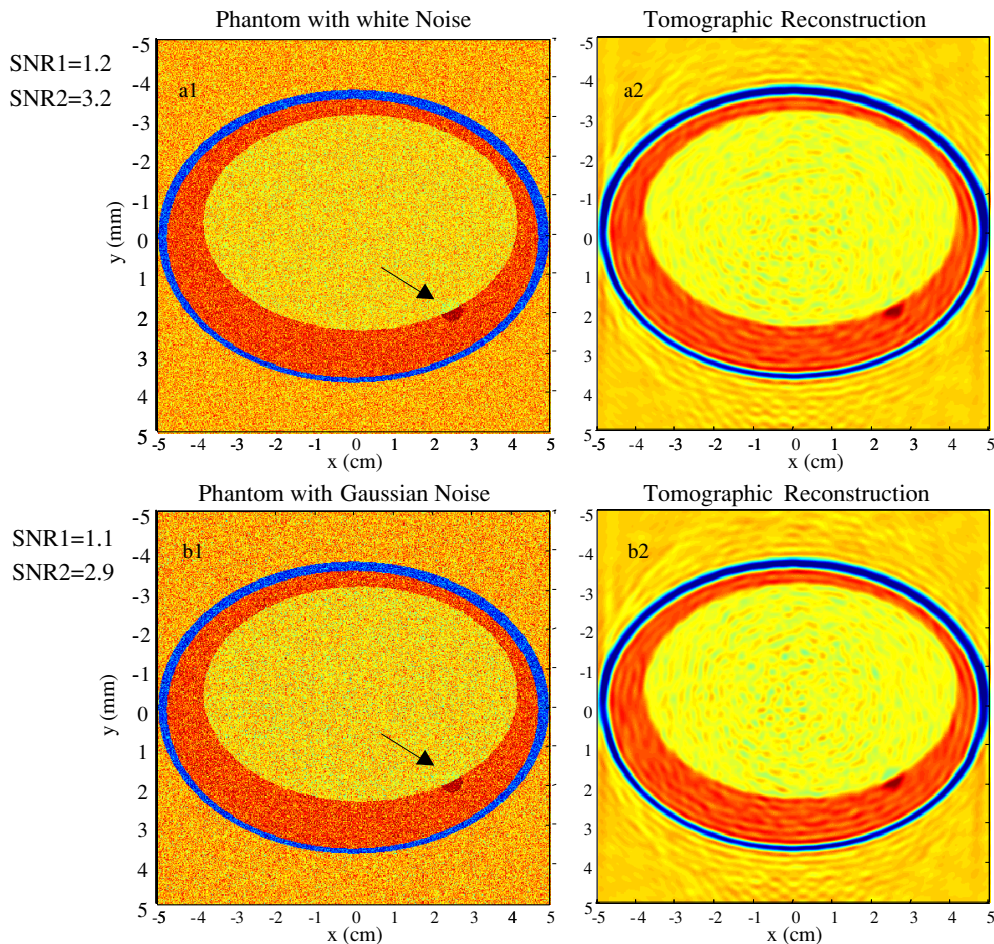


Figure 9. (a1) A tissue phantom with time variant white noise added. A signal-to-noise ratio of 1.2 was measured in the tissue (SNR1) and 3.2 in the fat (SNR2) with heating of heated 5 C. (a2) The reconstructed at 0.7 MHz. (b1) The same phantom with Gaussian noise measured at SNR1=1.1 and SNR2 = 2.9 and (b2) its reconstruction.

4. Discussion

This numeric study was aimed at determining whether a phase-contrast ultrasound-imaging technique could be applied to monitoring thermal heating in soft tissues such as the breast. Since phase-contrast imaging is sensitive to phase shifts that are a fraction of a wavelength, it was hypothesized that imaging could be performed at frequencies approximately one order of magnitude lower than standard diagnostic frequencies. The lower frequencies would make the beam far less susceptible to scattering, and would produce a stronger signal at the receiver. It was also believed that the signal strength would be greatly improved since the phase-contrast technique operates with a multi-cycle signal. Furthermore, dispersive coupling of the phase and the absorption are negligible in soft tissue at the reduced imaging frequencies, so the phase-contrast image was not expected to be distorted by absorption over the beam path.

Simulation results revealed an expected reduction in the spatial resolution, which was a tradeoff for going to lower frequencies. It is was therefore necessary to determine the lowest

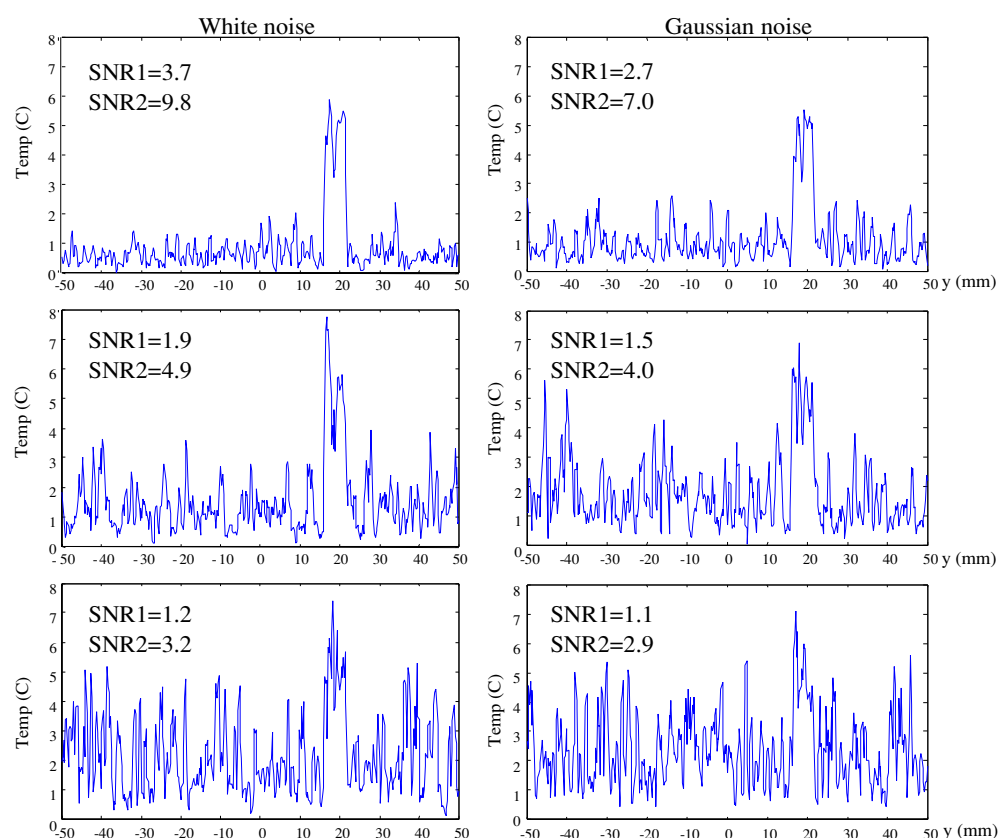


Figure 10. Cross-section of apparent temperature in tissue layers corresponding to figure 9 for increasing levels of white noise (left) and Gaussian noise (right).

possible frequencies that could still provide information about the tissue structure (tissue–fat layers) and temperature rise within dimensions expected in thermal breast applications. An imaging frequency of 0.7 MHz, was observed to allow a reconstruction resolution of about 2 mm^2 over the image plane, which is sufficient for thermal monitoring. If greater accuracy is necessary, it is also possible that the breast could be imaged at higher resolution using an alternative method such as CT or MRI to provide *a priori* knowledge of the tissue composition, and then the heating imaged with ultrasound. Additionally, a wavefront correction algorithm (Clement and Hynynen 2002) could be introduced to provide more accurate imaging.

Simulations of heating in homogeneous tissue, shown in figures 3 and 4, indicated that wavelengths larger than the FWHM of the heating profile were able to detect heating, but with image distortion that included an artificially reduced temperature amplitude and an artificially increased heating area. The physical origin of this bias may be explained in terms of a point spread function, and has a direct analogy to the blurring of spatial objects in optics. The simulations indicate that wavelengths larger than the heating diameter could be used for qualitative localization the focus of a therapeutic transducer but could not be used for quantitative measurement without further resolving the data.

While quantification of motion effects are beyond the scope of the present work, time-dependent motion is expected to produce blurring artefacts in the images, similar to that of

other techniques using backprojection kernels. Any change in temperature over the acquisition time will serve to distort the spatial frequency space as a function of angle, raising the question of whether this too will cause artefacts. However, simulation of this process, assuming a linear change in temperature of about 3° degrees, returned a value close to the average temperature over this period without causing any detectable further distortion of the image.

In our study, we also determined that a steady state heating could be produced in a targeted area and then the method could be used to identify the difference between fat and muscle or breast tissue (figure 7). We are presently investigating this use for identification of fat/tissue layers and for tumour detection. It may also be possible to acquire a series of images after heating to determine the heat capacity or thermal perfusion rate of a given tissue, providing a new tool for noninvasive imaging of a tissue's thermal properties.

The simulations further demonstrated that phase-contrast imaging in a region composed of both fat and tissue is possible, but that wavevector-domain reconstruction would be necessary in this situation in order to obtain even qualitative images of the heating. The temperature resolution on a physical system will ultimately depend on the signal-to-noise ratio experienced in the clinic. The goal of the present study was to determine the feasibility of the method, and to provide demonstration under ideal conditions to illustrate the approach. Further, it was assumed that the tissue was stationary and that the temperature was constant over the acquisition period.

Future work will require reconstruction under experimental conditions, to complement our previously reported preliminary experimental work in *ex vivo* tissues (King *et al* 2003). It is suggested that the application of the method in real tissue may be possible in breast tissue, where ultrasound transmission is possible. The model indicates that heat may be imaged in tissue fat interfaces. This is encouraging for possible application in the breast, which may contain a complex interleaving of fat and breast tissue.

References

- Banerjee P P and Poon T-C 1991 *Principles of Applied Optics* (New York: Aksen Associates Inc)
- Carson P L, Oughton T V, Hendee W R and Ahuja A S 1977 Imaging soft tissue through bone with ultrasound transmission tomography by reconstruction *Med. Phys.* **4** 302
- Chapelon J Y, Ribault M, Vernier F, Souchon R and Gelet A 1999 Treatment of localised prostate cancer with transrectal high intensity focused ultrasound *Eur. J. Ultrasound* **9** 31–8
- Clement G T 1999 Evaluation of transient and highly localized acoustic fields using acoustooptic phase contrast imaging. *PhD Thesis* Department of Physics U Rhode Island, USA
- Clement G T and Hynynen K 2000 Field characterization of therapeutic arrays through forward and backward planar projection *J. Acoust. Soc. Am.* **108** 441–6
- Clement G T and Hynynen K 2002 A noninvasive method for focusing ultrasound through the human skull *Phys. Med. Biol.* **47** 1219–36
- Clement G T, King R L and Hynynen K 2001 Feasibility of therapy monitoring using an acoustic camera *Proc. 1st Int. Workshop on the Application of HIFU in Medicine* vol 1, pp 32–4
- Clement G T and Letcher S V 1999 Phase-contrast optical imaging of transient acoustic signals *J. Acoust. Soc. Am.* **106** 2193(A)
- Cline H E, Hynynen K, Watkins R D, Adams W J, Schenck J F, Ettinger R H, Freund W R, Vetro J P and Jolesz F A 1995 Focused US system for MR imaging-guided tumour ablation *Radiology* **194** 731–7
- Dewey W C 1994 Arrhenius relationships from the molecule and cell to the clinic *Int. J. Hyperthermia* **10** 457–83
- Dines K A, Fry F J, Patrick J T and Gilmor R L 1981 Computerized ultrasound tomography of the human head: experimental results *Ultrason. Imaging* **3** 342–51
- Duck F A 1990 *Physical Properties of Tissue* (London: Academic)
- Ermert H, Keitmann O, Oppelt R, Granz B, Pesavento A, Vester M, Tillig B and Sander V 2000 A new concept for a real-time ultrasound transmission camera *IEEE Ultrasonics Symposium* pp 1611–14
- Fallone B G, Moran P R and Podgorsak E B 1982 Noninvasive thermometry with a clinical x-ray CT scanner *Med. Phys.* **9** 715–21

- Forbes M, Letcher S V and Stepanishen P R 1991 A wave vector, time-domain method of forward projecting time-dependent pressure fields *J. Acoust. Soc. Am.* **90** 2782–93
- Fry F J and Jethwa C P 1974 Ultrasonic transmission imaging using Gaussian noise source *J. Clin. Ultrasound* **2** 230
- Fry W J, Leichner G H, Okuyama D, Fry F J and Fry E K 1968 Ultrasonic visualization system employing new scanning and presentation methods *J. Acoust. Soc. Am.* **44** 1324–38
- Goodman J W 1968 *Introduction to Fourier Optics* (New York: McGraw-Hill)
- Green P S and Arditi M 1985 Ultrasonic reflex imaging *Ultrasound Imaging* **7** 201–14
- Green Ostrem J S and Whitehurst T K 1991 Combined reflection and transmission ultrasound imaging *Ultrasound Med. Biol.* **17** 283–9
- Green P S, Schaefer L F, Jones E D and Suarez J R 1973 A new high-performance ultrasonic camera *Acoustical Holography* ed P S Green (New York: Plenum Press)
- Hecht E 1987 *Optics* (Reading, MA: Addison-Wesley)
- Hentz V R, Green P S and Arditi M 1987 Imaging studies of the cadaver hand using transmission ultrasound *Skeletal Radiol.* **16** 474–80
- Hinkelman L M, Liu D-L, Waag R C, Zhu Q and Steinberg B D 1995 Measurement and correction of ultrasonic pulse distortion produced by the human breast *J. Acoust. Soc. Am.* **97** 1958–69
- Jenne J W, Bahner M, Spoo J, Huber P, Rastert R, Simiantonakis I, Lorenz W J and Debus J 1997 CT on-line monitoring of HIFU therapy 1997 *IEEE Ultrasonics Symposium Proceedings, An International Symposium* p 1377
- Kaveh M, Soumekh M and Greenleaf J F 1984 Signal processing for diffraction tomography *IEEE Trans. Sonics. Ultrasonics* **31** 230–9
- King R L, Clement G T, Maruvada S and Hynynen K 2003 Preliminary results using ultrasound transmission for image-guided thermal therapy *Ultrasound Med. Biol.* **29** 293–9
- Lasser M E 1997 A novel high speed, high resolution, ultrasound imaging system *Materials Research Society Symposium Proceedings Series* vol 503
- Lasser M E, Harrison G H and Agarwal M 1996 Acoustic Microscopy for 100% non-destructive semiconductor package evaluation *Proc. 1996 Int. Symp. Microelectronics* pp 82–6
- Lehman C D, Andre M P, Fecht B A, Johansen J M, Shelby R L and Shelby J O 2000 Through-transmission US applied to breast imaging *Acad. Radiol.* **7** 100–7
- Liu D-L and Waag R C 1994 Correction of ultrasonic wavefront distortion using backpropagation and a reference waveform method for time-shift compensation *J. Acoust. Soc. Am.* **96** 649–60
- Maas-Moreno R and Damianou C A 1996 Noninvasive temperature estimation in tissue via ultrasound echo-shifts. Part I. Analytical model *J. Acoust. Soc. Am.* **100** 2514–21
- Maas-Moreno R, Damianou C A and Sanghvi N T 1996 Noninvasive temperature estimation in tissue via ultrasound echo-shifts. Part II. *In vitro* study *J. Acoust. Soc. Am.* **100** 2522–30
- Marich K W, Zatz L M, Green P S, Suarez J R and Macovski A 1975a Real-time imaging with a new ultrasonic camera. Part I. *In vitro* experimental studies on transmission imaging of biological structures *J. Clin. Ultrasound* **3** 5–16
- Marich K W, Zatz L M, Green P S, Suarez J R and Macovski A 1975b Real-time imaging with a new ultrasonic camera. Part II. Studies in normal adults *J. Clin. Ultrasound* **3** 17–22
- McDannold N J and Jolesz F A 2000 Magnetic resonance image-guided thermal ablations *Top. Magn. Reson. Imaging* **11** 191–202
- McGough R J, Wang H, Ebbini E S and Cain C A 1994 Mode scanning: heating pattern synthesis with ultrasound phased arrays *Int. J. Hyperthermia* **10** 433–42
- Metherell A F, Spinak S and Pisa E J 1970 Temporal reference acoustic holography *Proc. 2nd Int. Symp. on Acoustical Holography* pp 69–86
- Nock L, Trahey G E and Smith S W 1989 Phase aberration correction in medical ultrasound using speckle brightness as a quality factor *J. Acoust. Soc. Am.* **85** 1819–33
- O'Donnell M and Flax S W 1988 Phase aberration measurements in medical ultrasound: Human studies *Ultrasound Imaging* **10** 1–11
- Opielinski K J and Gudra T 2000 Ultrasound transmission tomography image distortions caused by the refraction effect *Ultrasonics* **38** 424–9
- Pitts T A, Sagers A and Greenleaf J F 2001 Optical Phase Contrast Measurement of Ultrasonic Fields *IEEE Trans. Ultrason. Ferroelectr. Freq. Contr.* **48** 1686–94
- Pomeroy O H, Hynynen K, Singer S, Christian R, Frenna T H and Jolesz F A 1995 MR Imaging-guided focused US therapy for breast fibroadenomas: a feasibility study *Radiology* **197** 311–2
- Quesson B, de Zwart J A and Moonen C T 2000 Magnetic resonance temperature imaging for guidance of thermotherapy *J. Mag. Res. Imag.* **12** 525–33

- Sanghvi N T, Foster R S, Bihrlé R, Casey R, Uchida T, Phillips M H, Syrus J, Zaitsev A V, Marich K W and Fry F J 1999 Noninvasive surgery of prostate tissue by high intensity focused ultrasound: an updated report *Eur. J. Ultrasound* **9** 19–29
- Schafer M E 1988 Transducer characterization in inhomogeneous media using the angular spectrum method *PhD Thesis* Drexel University
- Schafer M E, Lewin P A and Reid J M 1987 Propagation Through Inhomogeneous Media Using the Angular Spectrum Method 1987 *IEEE Ultrasonics Symposium Proceedings* pp 943–6
- Seip R and Ebbini E S 1995 Noninvasive estimation of tissue temperature response to heating fields using diagnostic ultrasound *IEEE. Trans. Biomed. Eng.* **42** 828–39
- Sheljaskov T, Lerch R, Fuchs A and Schatzle U 1997 A phased array antenna for simultaneous thermotherapy and sonography 1997 *IEEE Ultrasonics Symposium Proceedings. An International Symposium* p 1701
- Stepanishen P R 1971 Transient radiation from pistons in an infinite planar baffle *J. Acoust. Soc. Am.* **49** 1629–38
- Stepanishen P R and Benjamin K C 1982 Forward and backward projection of acoustic fields using FFT methods *J. Acoust. Soc. Am.* **71** 803–12
- Stepanow B, Huber P, Brix G, Debus J, Bader R, van Kaick G and Lorenz W J 1995 Fast MRI temperature monitoring: application in focused ultrasound therapy of malignant tissue *in vivo Proc SMR 3rd Meeting* 1172
- Umemura S and Cain C A 1989 The sector-vortex phased array: acoustic fields synthesis for hyperthermia *IEEE Trans. Ultrason. Ferroelectr. Freq. Contr.* **36** 249–57
- Wadley H N G, Norton S J, Mauer F and Droney B 1986 Ultrasonic measurement of internal temperature distribution *Phil. Trans. R. Soc. Lond A* **320** 341–61
- Weigel J P and Cartee R E 1983 Preliminary Study on the Use of Ultrasonic Transmission Imaging to Evaluate the Hip Joint in the Immature Dog *Ultrasound Med. Biol.* **9** 371–8
- Wells P N T 2000 Advances in ultrasound: from microscanning to telerobotics *Br. J. Radiol.* **73** 1138–47
- Whitman R L, Korpel A and Ahmed M 1972 Novel technique for real-time depth-gated acoustic image holography *Appl. Phys. Lett.* **20** 370–1
- Zatz L M 1975 Initial clinical evaluation of a new ultrasonic camera *Radiology* **117** 399–404
- Zhu Q and Steinberg B D 1997 Modeling and correction of incoherent wavefront distortion *Int. J. Imaging. Syst. Technol.* **8** 322–35